Enhancement of tunneling magnetoresistance by inserting a diffusion barrier in $L1_0$-FePd perpendicular magnetic tunnel junctions

De-Lin Zhang, Karl B. Schliep, Ryan J. Wu, P. Quarterman, Danielle Reifsnyder Hickey, Yang Lv, Xiaohui Chao, Hongshi Li, Jun-Yang Chen, Zhengyang Zhao, Mahdi Jamali, K. Andre Mkhoyan, and Jian-Ping Wang

Citation: Appl. Phys. Lett. **112**, 152401 (2018); doi: 10.1063/1.5019193
View online: https://doi.org/10.1063/1.5019193
View Table of Contents: http://aip.scitation.org/toc/apl/112/15
Published by the American Institute of Physics

Enhancement of tunneling magnetoresistance by inserting a diffusion barrier in $L1_0$-FePd perpendicular magnetic tunnel junctions

De-Lin Zhang,[1] Karl B. Schliep,[2] Ryan J. Wu,[2] P. Quarterman,[1] Danielle Reifsnyder Hickey,[2] Yang Lv,[1] Xiaohui Chao,[1] Hongshi Li,[2] Jun-Yang Chen,[1] Zhengyang Zhao,[1] Mahdi Jamali,[1] K. Andre Mkhoyan,[2] and Jian-Ping Wang[1,a)]
[1]*Department of Electrical and Computer Engineering, University of Minnesota, Minneapolis, Minnesota 55455, USA*
[2]*Department of Chemical Engineering and Materials Science, University of Minnesota, Minneapolis, Minnesota 55455, USA*

(Received 12 December 2017; accepted 13 February 2018; published online 9 April 2018)

We studied the tunnel magnetoresistance (TMR) of $L1_0$-FePd perpendicular magnetic tunnel junctions (p-MTJs) with an FePd free layer and an inserted diffusion barrier. The diffusion barriers studied here (Ta and W) were shown to enhance the TMR ratio of the p-MTJs formed using high-temperature annealing, which are necessary for the formation of high quality $L1_0$-FePd films and MgO barriers. The $L1_0$-FePd p-MTJ stack was developed with an FePd free layer with a stack of FePd/X/$Co_{20}Fe_{60}B_{20}$, where X is the diffusion barrier, and patterned into micron-sized MTJ pillars. The addition of the diffusion barrier was found to greatly enhance the magneto-transport behavior of the $L1_0$-FePd p-MTJ pillars such that those without a diffusion barrier exhibited negligible TMR ratios (<1.0%), whereas those with a Ta (W) diffusion barrier exhibited TMR ratios of 8.0% (7.0%) at room temperature and 35.0% (46.0%) at 10 K after post-annealing at 350 °C. These results indicate that diffusion barriers could play a crucial role in realizing high TMR ratios in bulk p-MTJs such as those based on FePd and Mn-based perpendicular magnetic anisotropy materials for spintronic applications. *Published by AIP Publishing*. https://doi.org/10.1063/1.5019193

Recently, using materials with perpendicular magnetic anisotropy (PMA) to develop spintronic devices has attracted great interest for realizing ultra-low power consumption spin memory and logic devices.[1–6] The key building block of these devices is the magnetic tunnel junctions (MTJs). To preserve commercial viability, MTJ-based devices must maintain the industry standard of 10 years of reliable storage ($\Delta \geq 60$) and a low reversal current density for current-induced magnetization switching.[7,8] This requires that the ferromagnetic layer must possess both a large PMA energy (K_u) and a low damping constant (α).[9–11] Recently, interfacial PMA materials have shown considerable progress in the application of spin-transfer-torque magnetic random access memory (STT-MRAM).[12–15] However, because of their relatively low PMA value ($K_u \sim 2$–5×10^6 erg/cm^3),[2,11,16,17] they may not fully satisfy the scaling demands required for next-generation memory and logic devices. The $L1_0$-phase of FePd is a promising material candidate for spintronic devices due to its large theoretical PMA ($K_u \sim 2 \times 10^7$ erg/cm^3), low α, and low processing temperature.[18–21] $L1_0$-FePd has recently been experimentally verified to have $\alpha \sim 0.002$ and $K_u \sim 1.3$–1.4×10^7 erg/cm^3 (Refs. 2, 22, and 23) and, as reported by Naganuma *et al.*,[24] has demonstrated a 27.0% room temperature (RT) tunnel magnetoresistance (TMR) ratio in partially perpendicular MTJs (p-MTJs) with an in-plane reference layer.

In addition, spintronic devices must sustain operation reliability for processing temperature as high as 400 °C for their integration with existing CMOS technologies [the standard back-end-of-line (BEOL) process].[25] Based on this requirement, the magnetic properties of a material exhibiting PMA should be thermally stable at an annealing temperature of 400 °C. Unfortunately, Pd-based PMA devices are, however, currently hindered by Pd diffusion, which results in penetration of Pd into adjacent layers during the thermal treatment process, dramatically reducing the tunnel magnetoresistance (TMR) ratio.[26] Typically, to solve the element diffusion problem, the inserting layer (named as the diffusion barrier) was introduced to block the element diffusion which protects the devices with the high-temperature thermal treatment process.[27–30] Forming full stack p-MTJs with FePd and solving the Pd diffusion, however, are more difficult and have not been reported so far due to the need for high-temperature annealing that crystallizes both the fixed and free layers. In this letter, we design the full p-MTJ stack with the FePd free layer and the $[Co/Pd]_n$ reference layer, solve the Pd diffusion issue, and enhance the TMR ratio in FePd p-MTJs by inserting a diffusion barrier between the FePd and $Co_{20}Fe_{60}B_{20}$ (CoFeB) layers.[31] These experimental results demonstrate that diffusion barriers can be used to block Pd diffusion and enhance the TMR ratio of $L1_0$-FePd p-MTJ devices during high-temperature thermal treatments (post-annealing at 350 °C).

All samples were prepared under ultra-high vacuum (base pressure $<5.0 \times 10^{-8}$ Torr) using the standard magnetron sputtering systems. All metal layers were deposited by a DC source under an Ar pressure of 2.0 mTorr, except for FePd at 4.5 mTorr. The MgO barrier layer was deposited by an RF source at an Ar pressure of 1.5 mTorr. The FePd thin films were prepared with a Cr/Pt seed layer by co-sputtering of the Fe and Pd targets. The composition of FePd is evaluated to be $Fe_{53}Pd_{47}$ by using Rutherford backscattering spectrometry (RBS). The crystalline structure and magnetic properties of the FePd thin

a)Author to whom correspondence should be addressed: jpwang@umn.edu

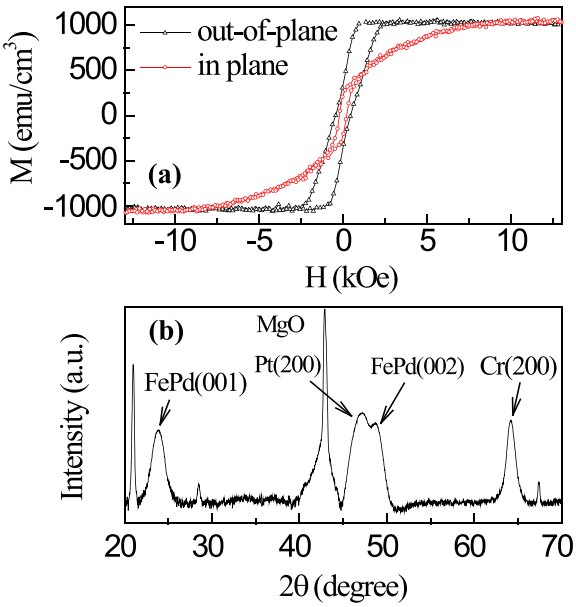

FIG. 1. (a) Room-temperature magnetization hysteresis (M-H) loops for a FePd single-layer thin film with the stacking of Cr(15 nm)/Pt(4 nm)/FePd(6 nm)/Ta(5 nm) deposited on a (100) MgO single-crystalline substrate. (b) The out-of-plane XRD pattern of a 6-nm-thick FePd single-layer thin film.

films were characterized using X-ray diffraction (XRD) and a Physical Property Measurement System (PPMS) with a vibrating sample magnetometer (VSM) module, respectively. An aberration-corrected FEI Titan G2 60–300 scanning transmission electron microscope (STEM) operated at 200 kV and equipped with a Super-X system was used for high-angle annular dark-field (HAADF)-STEM imaging and energy-dispersive X-ray spectroscopy (EDX) of the FePd p-MTJ stack. During the experiment, the nominal STEM probe convergence angle was 45 mrad with an electron beam current of ~200 pA. The full p-MTJ stacks have a structure of MgO sub./Cr(15)/Pt(5)/FePd(6)/**X**(0.8)/CoFeB(1.3)/MgO(2)/CoFeB(1.3)/Ta(0.7)/[Pd(0.7)/Co(0.3)]$_5$/Pd(5)/Ta(5) (X = Ta or W) (the number is the film thickness in nanometers). Additionally, these stacks were made with and without a diffusion barrier for comparison. Afterward, the p-MTJ stacks were patterned using optical lithography and an Ar-ion milling method into micron-sized MTJ pillars with diameters ranging from 4 μm to 20 μm. Subsequently, all MTJ devices were annealed at 350 °C for 30 minutes by the rapid thermal annealing (RTA) process. The magneto-transport properties of these p-MTJs were tested at various temperatures by a four-probe technique using a PPMS.

The magnetic behaviour and crystalline structure of the as-deposited 6-nm-thick FePd thin films were first investigated, and the results are plotted in Fig. 1. From the M-H loops, the easy axis of the FePd thin films is found to be perpendicular to the plane of the film with a saturation field (H_K) of ~ 8.0 kOe (from the in-plane M-H loop), indicating that the FePd thin films possess large PMA. A saturation magnetization (M_S) was calculated to be 1020 ± 30 emu/cm^3, which is similar to the bulk value (~1100 emu/cm^3).[32] Following the equation $K_u = \frac{M_S H_K}{2} + 2\pi M_S^2$,[19] the PMA energy ($K_u$) was determined to be ~$1.06 \times 10^7$ erg/cm^3 based on the H_K and M_S values of FePd thin film. The anisotropy energy per area (K_{eff}.t_{FM}) (here, K_{eff} is the effective anisotropy and t_{FM} is the thickness of the ferromagnetic layer) for the 6-nm-thick FePd thin film is calculated to be ~2.5 erg/cm^2, which is larger than that of the 400 °C post-annealed W/CoFeB/MgO interfacial PMA stack (K_{eff}.t_{FM} ~ 0.8–1.6 erg/cm^2).[33,34] This property of the FePd thin film could satisfy the requirement of p-MTJ devices for ultrahigh-density MRAM. Furthermore, the appearance of the (001) and (002) peaks of the FePd thin film indicates that its crystalline structure is the high-quality $L1_0$ structure (AuCu-I) from the out-of-plane XRD patterns, as shown in Fig. 1(b). In addition, the Cr/Pt seed layer is used to induce the (001) texture and reduces the lattice mismatch between FePd and MgO substrates. Similarly, the (002) peak of Cr and the (200) peak of Pt indicate that the Cr/Pt seed layer has good texture on the MgO (001) single-crystalline substrate.

The full p-MTJ stack was designed, based on the high-quality FePd thin films, as shown in Fig. 2(a). In this full p-MTJ stack, the Ta or W layer is inserted between FePd and CoFeB layers to form a free layer (named as the FePd free layer). A CoFeB/Ta/[Co/Pd]$_n$ stack is used as a reference layer (named as the [Co/Pd]$_n$ reference layer). The FePd free layer with a Ta diffusion barrier was post-annealed at 350 °C for 30 minutes in a high-vacuum furnace. The out-of-plane M-H loop is shown in Fig. 2(b). From the M-H loop, we can see that the FePd free layer with a Ta diffusion barrier exhibits a single switch—indicating that the FePd layer ferromagnetically couples with the CoFeB layer through the 0.8-nm-thick Ta diffusion barrier layer. The FePd free layer with the W

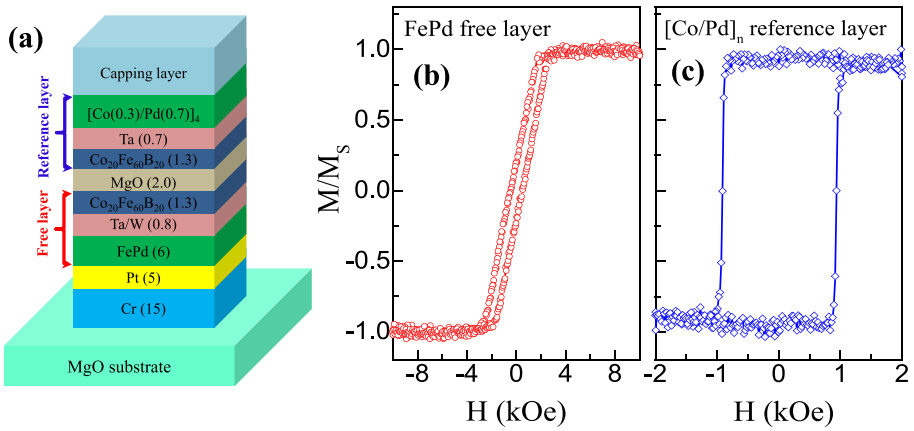

FIG. 2. (a) A schematic illustration of the full FePd perpendicular magnetic tunnel junction stacks with Ta or W diffusion barriers: the FePd free layer with a stack of FePd/X/CoFeB (X = Ta or W) and the [Co/Pd]$_n$ reference layer with a stack of [Co/Pd]$_n$/Ta/CoFeB. The room-temperature out-of-plane magnetization hysteresis (M-H) loops of (b) the FePd free layer and (c) the [Co/Pd]$_n$ reference layer. The inserted Ta layer is designed as a diffusion barrier.

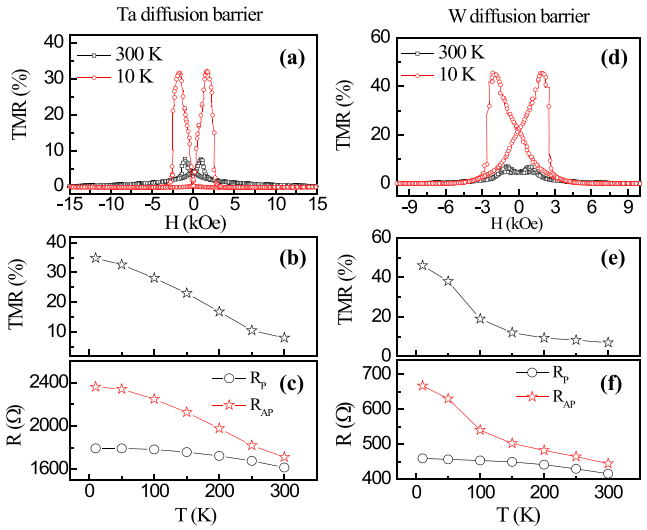

FIG. 3. (a) and (d) Magnetoresistance vs. external magnetic field (MR-H) curves measured at 10 K and 300 K of the micron-sized FePd p-MTJ devices with the Ta and W diffusion barriers, respectively. The junctions are annealed by rapid thermal anneal (RTA) at 350 °C for 30 minutes. Temperature dependencies of (b) and (e) TMR ratio and (c) and (f) resistance of the parallel state (open stars) and the antiparallel state (open circles) for Ta and W diffusion barriers, respectively.

diffusion barrier shows the same PMA property as the FePd free layer with the Ta diffusion barrier (not shown here). The optimized thickness of the Ta and W spacers for the strongest ferromagnetic coupling is less than ~0.7 nm,[34,35] which is thinner than that of the Ta and W diffusion barriers in FePd p-MTJ stacks. Figure 2(c) shows the M-H loop of the $[Co/Pd]_n$ reference layer after post-annealing at 350 °C for 30 minutes. The square shape and a large coercivity (H_c) of ~1200 Oe suggest good PMA and thermal stability.

To study the magneto-transport properties, the full p-MTJ stacks with/without the Ta and W diffusion barriers were patterned into the micron-sized MTJ pillars. First, TMR of these as-deposited FePd p-MTJ devices was obtained, ~6.0% and ~3.0% room temperature (RT) TMR ratios in the micron-sized FePd p-MTJs without and with the Ta diffusion barrier, respectively. After annealing at 350 °C for 30 minutes, however, the p-MTJ devices without the diffusion barrier showed an almost zero RT TMR ratio—suggesting that Pd in the FePd layer diffuses into the CoFeB layer or the MgO barrier. Figure 3(a) shows the TMR vs. external magnetic field (TMR-H) curve of the FePd p-MTJ devices with the Ta diffusion barrier. The TMR ratio is calculated to be ~8.0% at 300 K. Additionally, the FePd p-MTJ devices with the Ta diffusion barrier do not show the obviously parallel (p)-antiparallel (AP) state magnetization switching with a plateau in the high-resistance state but rather an angular dependence of the TMR effect in the P-AP switching.[36] The main reason could be the multi-domain nature of the FePd bottom free layer and the strong dipole coupling between the bottom free layer and the top reference layer. To investigate the mechanism of magneto-transport, the temperature dependence of the TMR ratios of the FePd p-MTJ devices with the Ta diffusion barrier was measured, as shown in Fig. 3(b). Upon decreasing the temperature from 300 K to 10 K, the TMR ratios gradually increased to ~35.0%, which is four times larger than that of the RT TMR ratio. The different TMR ratios between RT and low-temperature observed are due to elemental diffusion (boron) or the oxidation of the ferromagnetic layer (Co or Fe) at the CoFeB/MgO interface during the high-temperature post-annealing, which can strongly affect the magneto-transport of these p-MTJs.[37] In addition, the coherent tunneling behavior originating from the quality of the MgO tunnel barrier shows that the resistance of MTJ in the P state is relatively constant and the resistance of MTJ in the AP state exhibits a strong temperature dependence.[38] By measuring the resistance of the P and AP states as a function of the temperature, we can deduce whether the coherent tunneling behavior is observed in FePd p-MTJ devices. Figure 3(c) shows the temperature dependence of the resistance of the P and AP states for FePd p-MTJs with the Ta diffusion barrier post-annealed at 350 °C. We observed that the resistance in the AP state exhibits a strong temperature dependence, whereas the resistance in the P state slightly decreases with increasing temperature. This implies that the coherent tunneling behavior has not been observed in the FePd p-MTJ devices. This may also be the reason why the TMR ratio is still low in FePd p-MTJ devices at RT.

The same investigation was performed to understand the magneto-transport behaviour of the FePd p-MTJ devices with a W diffusion barrier, and the results are shown in Figs. 3(d)–3(f). The TMR ratios of the FePd P-MTJ devices are calculated to be ~7.0% at RT and ~46.0% at 10 K after post-annealing the devices at 350 °C for 30 min as plotted in Fig. 3(d). We do not observe a plateau in the high-resistance state at RT or low-temperature rather than an angular dependence of the P-AP switching in this p-MTJ. Compared to the MR-H loop at 300 K, when the temperature goes down to 10 K, the TMR ratios dramatically increase from ~7.0% to ~46.0% as shown in Fig. 3(e), which is an increase by a factor of 7. Except that the reason for the surface magnetization instability and/or magnetic impurities in the MgO barrier, the other possible reason is that the W material has a good thermal stability compared to a Ta diffusion barrier, so the W diffusion barrier can block Pd diffusion efficiently.[39] The temperature dependence of resistance in the P and AP states was plotted, as shown in Fig. 3(f). Note that the resistance change as a function of the temperature in FePd p-MTJ devices with the W diffusion barrier shows the same trend as that in FePd p-MTJ devices with the Ta diffusion barrier.

Considering the sensitivity of the FePd p-MTJ stack to the thickness, crystallinity, and interfacial characteristics of its many layer components, it is advantageous to characterize the device structure in cross-section to analyze each component. Following the study of the magnetic properties and p-MTJ device performance, the FePd p-MTJ stack with the Ta barrier was thinned cross-sectionally into an electron-transparent lamella (~50 nm thick) using a focused ion beam (FIB) and, subsequently, inserted into a scanning transmission electron microscope (STEM) for characterization. Figure 4(a) shows cross-sectional annular dark-field (ADF)-STEM and bright field (BF)-STEM images of the FePd p-MTJ stack with the Ta diffusion barrier [for ADF-STEM, the difference in intensity between each layer is due to atomic number (Z)-contrast]. All layers of the FePd p-MTJ stack, except the top native TaO_x layer, display crystalline fringes in one or both images, which

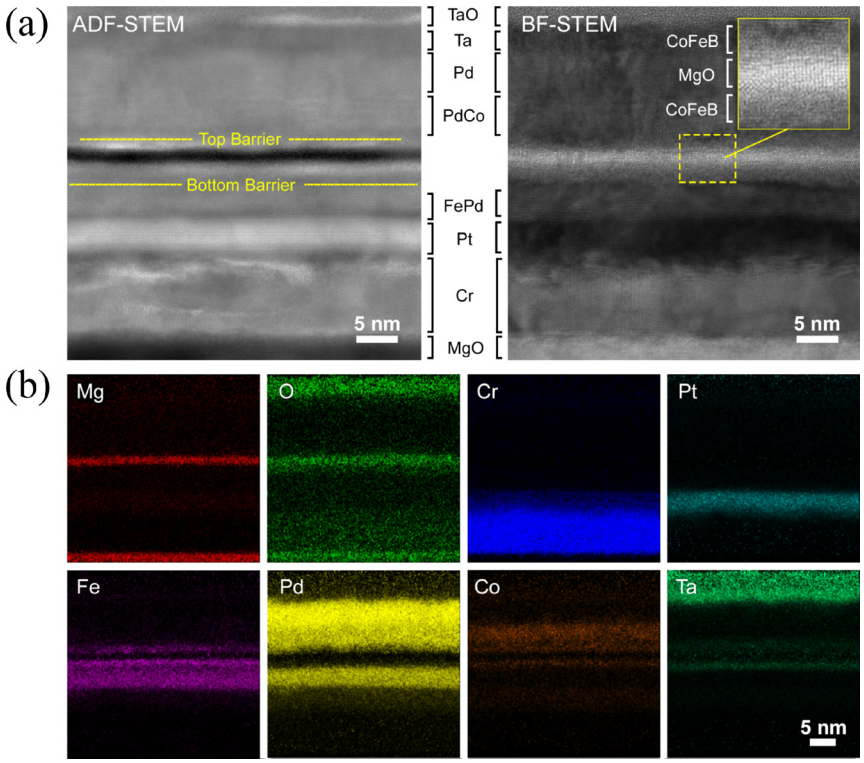

FIG. 4. (a) ADF-STEM and BF-STEM images of the FePd p-MTJ device with a Ta diffusion barrier in cross-section. The locations of the Ta diffusion barriers in the device are denoted in the ADF-STEM image. The inset in the BF-STEM image shows a magnified view of MgO and its surrounding CoFeB layers. (b) STEM-EDX elemental maps of Mg, O, Cr, Pt, Fe, Pd, Co, and Ta. The EDX signal was acquired by scanning the electron probe across the sample area shown in (b) continuously for 25 minutes at an electron beam current of ~200 pA.

shows that the sample is entirely crystalline. In particular, the MgO tunnel barrier layer shows a relatively high-quality crystalline structure. The elements of these crystalline layers were identified using energy dispersive X-ray (EDX) spectroscopy, presented here as elemental maps [Fig. 4(b)]. The location of each layer of the p-MTJ based on the EDX maps is consistent with the device schematic shown in Fig. 2(a). Combined with Figs. 4(a) and 4(b), it is clearly found that the Cr seed layer exhibits slight diffusion into Pt but that a very smooth Pt/FePd interface exists. In addition, it is worth noting that the Ta barriers on both the free and reference layer sides of the p-MTJ are visible in the Ta elemental map, but it is difficult to identify Ta diffusion due to its small thickness.

In conclusion, we investigated the magneto-transport in the micron-sized FePd p-MTJ devices. The thermal stability of FePd p-MTJs was enhanced by introducing thin Ta and W diffusion barriers between the FePd and CoFeB layers. Compared to the FePd p-MTJs without the diffusion barrier (TMR is almost "zero"), 8.0% and 7.0% RT TMR ratios have been obtained in FePd p-MTJs with the Ta and W diffusion barriers, respectively. Additionally, the resistance of the P and AP states in the FePd p-MTJs with a W diffusion barrier showed a strong temperature dependence compared to those of FePd p-MTJs with a Ta diffusion barrier, which could be due to the better thermal stability of W than Ta. In addition, novel and multilayer diffusion barriers should be explored to pursue high TMR ratios in p-MTJs, which will satisfy the demands of semiconductor processing.

This work was supported by C-SPIN, one of the six centers of STARnet, a Semiconductor Research Corporation program, sponsored by MARCO and DARPA. Parts of this work were performed at the University of Minnesota Nanofabrication Center, which receives partial support from NSF through the NNIN program, and the Characterization Facility, which is a member of the NSF-funded Materials Research Facilities Network via the MRSEC program.

[1]H. Meng and J. P. Wang, Appl. Phys. Lett. **88**, 172506 (2006).
[2]S. Ikeda, K. Miura, H. Yamamoto, K. Mizunuma, H. D. Gan, M. Endo, S. Kanai, J. Hayakawa, F. Matsukura, and H. Ohno, Nat. Mater. **9**, 721 (2010).
[3]W.-G. Wang, M. Li, S. Hageman, and C. L. Chien, Nat. Mater. **11**, 64 (2012).
[4]A. D. Kent and D. C. Worledge, Nat. Nanotechnol. **10**, 187 (2015).
[5]G. Yu, P. Upadhyaya, Y. Fan, J. G. Alzate, W. Jiang, K. L. Wong, S. Takei, S. A. Bender, L.-T. Chang, Y. Jiang, M. Lang, J. Tang, Y. Wang, Y. Tserkovnyak, P. K. Amiri, and K. L. Wang, Nat. Nanotechnol. **9**, 548 (2014).
[6]P. Li, T. Liu, H. Chang, A. Kalitsov, W. Zhang, G. Csaba, W. Li, D. Richardson, A. DeMann, G. Rimal, H. Dey, J. S. Jiang, W. Porod, S. B. Field, J. Tang, M. C. Marconi, A. Hoffmann, O. Mryasov, and M. Wu, Nat. Commun. **7**, 12688 (2016).
[7]S. Yakata, H. Kubota, T. Sugano, T. Seki, K. Yakushiji, A. Fukushima, S. Yuasa, and K. Ando, Appl. Phys. Lett. **95**, 242504 (2009).
[8]H. Sato, E. C. I. Enobio, M. Yamanouchi, S. Ikeda, S. Fukami, S. Kanai, F. Matsukura, and H. Ohno, Appl. Phys. Lett. **105**, 062403 (2014).
[9]K. L. Wang, J. G. Alzate, and P. K. Amiri, J. Phys. D: Appl. Phys. **46**, 074003 (2013).
[10]G. Han, J. Huang, C. H. Sim, T. Michael, and S. T. Lim, J. Phys. D: Appl. Phys. **48**, 225001 (2015).
[11]S. Iihama, S. Mizukami, H. Naganuma, M. Oogane, Y. Ando, and T. Miyazaki, Phys. Rev. B **89**, 174416 (2014).
[12]D. C. Worledge, G. Hu, D. W. Abraham, J. Z. Sun, P. L. Trouilloud, J. Nowak, S. Brown, M. C. Gaidis, E. J. O'Sullivan, and R. P. Robertazzi, Appl. Phys. Lett. **98**, 022501 (2011).
[13]P. K. Amiri, Z. M. Zeng, J. Langer, H. Zhao, G. Rowlands, Y.-J. Chen, I. N. Krivorotov, J.-P. Wang, H. W. Jiang, J. A. Katine, Y. Huai, K. Galatsis, and K. L. Wang, Appl. Phys. Lett. **98**, 112507 (2011).
[14]H. Meng, R. Sbia, M. A. K. Akhtar, R. S. Liu, V. B. Naik, and C. C. Wang, Appl. Phys. Lett. **100**, 122405 (2012).
[15]K. Mizunuma, M. Yamanouchi, H. Sato, S. Ikeda, S. Kanai, F. Matsukura, and H. Ohno, Appl. Phys. Express **6**, 063002 (2013).

[16]Y. K. Takahashi, Y. Miura, R. Choi, T. Ohkubo, Z. C. Wen, K. Ishioka, R. Mandal, R. Medapalli, H. Sukegawa, S. Mitani, E. E. Fullerton, and K. Hono, Appl. Phys. Lett. **110**, 252409 (2017).
[17]H. Sato, M. Yamanouchi, K. Miura, S. Ikeda, H. D. Gan, K. Mizunuma, R. Koizumi, F. Matsukura, and H. Ohno, Appl. Phys. Lett. **99**, 042501 (2011).
[18]F. Bonell, S. Murakami, Y. Shiota, T. Nozaki, T. Shinjo, and Y. Suzuki, Appl. Phys. Lett. **98**, 232510 (2011).
[19]S. Iihama, A. Sakuma, H. Naganuma, M. Oogane, T. Miyazaki, S. Mizukami, and Y. Ando, Appl. Phys. Lett. **105**, 142403 (2014).
[20]H.-R. Lee, K. Lee, J. Cho, Y.-H. Choi, C.-Y. You, M.-H. Jung, F. Bonell, Y. Shiota, S. Miwa, and Y. Suzuki, Sci. Rep. **4**, 6548 (2014).
[21]P. V. Ong, N. Kioussis, P. K. Amiri, J. G. Alzate, K. L. Wang, G. P. Carman, J. Hu, and R. Wu, Phys. Rev. B **89**, 094422 (2014).
[22]S. Iihama, A. Sakuma, H. Naganuma, M. Oogane, S. Mizukami, and Y. Ando, Phys. Rev. B **94**, 174425 (2016).
[23]S. Iihama, M. Khan, H. Naganuma, M. Oogane, T. Miyazaki, S. Mizukami, and Y. Ando, J. Magn. Soc. Jpn. **39**, 57 (2015).
[24]H. Naganuma, G. Kim, Y. Kawada, N. Inami, K. Hatakeyama, S. Iihama, K. M. N. Islam, M. Oogane, S. Mizukami, and Y. Ando, Nano Lett. **15**, 623 (2015).
[25]A. J. Annunziata, P. L. Trouilloud, S. Bandiera, S. L. Brown, E. Gapihan, E. J. O'Sullivan, and D. C. Worledge, J. Appl. Phys. **117**, 17B739 (2015).
[26]V. Garcia-Vazquez, Y. J. Chang, A. Canizo-Cabrera, A. Garzon-Roman, and T. Wu, Jpn. J. Appl. Phys., Part 1 **55**, 023001 (2016).
[27]Z. Zhang, S. Cardoso, P. P. Freitas, X. Batlle, P. Wei, N. Barradas, and J. C. Soares, J. Appl. Phys. **89**, 6665 (2001).
[28]C.-S. Yoo, H. D. Jeong, J. H. Lee, C. S. Yoon, C. K. Kim, J. H. Yuh, Y. Ando, H. Kubota, and T. Miyazaki, IEEE Trans. Magn. **38**, 2715 (2002).
[29]Y. Fukumoto, K. Shimura, A. Kamijo, S. Tahara, and H. Yoda, Appl. Phys. Lett. **84**, 233 (2004).
[30]G. Hu, T. Topuria, P. M. Rice, J. Jordan-Sweet, and D. C. Worledge, IEEE Magn. Lett. **4**, 3000104 (2013).
[31]M. T. Rahman, A. Lyle, G. Hu, W. J. Gallagher, and J.-P. Wang, J. Appl. Phys. **109**, 07C709 (2011).
[32]D. Weller, A. Moser, L. Folks, M. E. Best, W. Lee, M. F. Toney, M. Schwickert, and J.-U. Thiele, IEEE Trans. Magn. **36**, 10 (2000).
[33]D. M. Lattery, D. Zhang, J. Zhu, J. P. Wang, and X. Wang, "Low Gilbert damping constant in perpendicularly magnetized W/CoFeB/MgO films with high thermal stability," preprint arXiv:1709.07483.
[34]J. H. Kim, J. B. Lee, G. G. An, S.-M. Yang, W.-S. Chung, H.-S. Park, and J.-P. Hong, Sci. Rep. **5**, 16903 (2015).
[35]C.-W. Cheng, T.-I. Cheng, C. H. Shiue, C.-L. Weng, Y.-C. Tsai, and G. Chern, IEEE Trans. Magn. **49**, 4433 (2013).
[36]T. Kubota, M. Araidai, S. Mizukami, X. Zhang, Q. Ma, H. Naganuma, M. Oogane, Y. Ando, M. Tsukada, and T. Miyazaki, Appl. Phys. Lett. **99**, 192509 (2011).
[37]Q. L. Ma, T. Kubota, S. Mizukami, X. M. Zhang, H. Naganuma, M. Oogane, Y. Ando, and T. Miyazaki, Phys. Rev. B **87**, 184426 (2013).
[38]S. Yuasa, A. Fukushima, H. Kubota, Y. Suzuki, and K. Ando, Appl. Phys. Lett. **89**, 042505 (2006).
[39]K.-M. Chang, T.-H. Yeh, I.-C. Deng, and C.-W. Shih, J. Appl. Phys. **82**, 1469 (1997).